Project Proposal

Raluca Pantilie

December 2021

Abstract

This project aims to develop understanding of type II superconductors by simulating the melting of a mixed state and training an image classification algorithm to label intermediary states. This document provides an overview of the relevant development of superconductivity, with a focus on the Ginzburg and Landau theory and type II superconductors. The forces acting on vortices used in the simulations are analysed ,furthermore appropriate equations of motion are described. Using the aforementioned equations, benchmark simulations are used to check for proper implementation. Finally, the main project is outlined, including its present state and future development.

1 Overview of superconductivity

In 1911 H. Kamerlingh Onnes measured the resistivity of mercury at low temperatures, which was found to drop to zero under a critical temperature of 4.15K [1, 2]. This effect was named superconductivity. However, this result could be the due to the resistivity falling below the sensitivity of the equipment. To check for this, a current was initiated in a superconducting ring and left to flow. The resulting magnetic field was observed to stay constant for a year [1]. Thus, perfect conductivity was firmly proven to be a characteristic of superconductivity. Further, experiments showed this state to appear in a variety of metals [3], proving it to be fairly widespread.

Alongside explorations of perfect conductivity in superconductors, other characteristics were found. Just a year after his discovery, H. Onnes found that a strong magnetic field breaks the superconductive state [2]. Also, in 1933 Meissner and Ochsenfeld found this state to exhibit perfect diamagnetism (also known as the Meissner effect). This phenomenon, affects a superconductor in an external magnetic field, which is expelled from the bulk of the material. But, on its surface, the magnetic field penetrates in a thin layer [1, 2, 3].

The first theoretical framework was developed by the London brothers via the London equations. They postulated that perfect conductivity is caused by a concentration,

n_s, of superconducting electrons (electrons with no scattering term) [1]. The London equations predicted the depth of penetration of a magnetic field in a superconductor (λ) [2], as well as its exponential decay [1, 4].

A better understanding of superconductivity was developed by Ginzburg and Landau (GL theory). They introduced a pseudowavefunction $\psi(\mathbf{r})$, such that $|\psi(\mathbf{r})|^2 = n_s$. They also performed an expansion of the free-energy density with respect to $|\psi(\mathbf{r})|^2$ [1, 2, 3]. The expansion was done close to the critical temperature T_c in order to ensure that $\psi(\mathbf{r})$ is small enough for the high order terms to be excluded. Noting that, when $\psi = 0$ the free-energy density is equal to that of a normal (non-superconducting) material, which results in

$$f_s = f_n + \alpha|\psi(\mathbf{r})|^2 + \beta|\psi(\mathbf{r})|^4.$$

However, this equation neglects any applied magnetic field or spatial variation of ψ. A more general equation is

$$f_s = f_n + \alpha|\psi(\mathbf{r})|^2 + \beta|\psi(\mathbf{r})|^4 + \frac{1}{2m^*}|(\frac{h}{i}\nabla - \frac{e^*}{c}\mathbf{A})\psi|^2, \tag{1}$$

where m^* and e^* are, respectively, the mass and charge of the superconductive electrons.

The Ginzburg-Landau equations represent the minimization of the free-energy density with respect to ψ and $\mathbf{A}$ [5] . Calculating the Ginzburg-Landau equations derived from equation 1 for a normalized wavefunction (f) with no external field ($\mathbf{A} = 0$) results in

$$\frac{\hbar^2}{2m^*|\alpha|}\frac{d^2f}{dx^2} + f - f^3 = 0, \tag{2}$$

which can be used to define the characteristic length, ξ, as follows

$$\xi^2 = \frac{\hbar^2}{2m^*|\alpha|}.$$

Solving equation 2 results in

$$f = Ce^{\pm\sqrt{2}x/\xi} - 1,$$

which shows that the characteristic length controls the decay of a small disturbance in $\psi(\mathbf{r})$[1].

Now there are two lengths controlling the behaviour of the material, the penetration depth λ, and the characteristic length, ξ. They can be combined to form the dimensionless Ginzburg-Landau parameter, κ, since

$$\kappa = \frac{\lambda}{\xi}.$$

Initially, the assumption was that κ was very small. This revealed a sharp loss in superconductive properties of the material at a field Hc_1. The behaviour was not expected to change drastically in the case of large κ values [1].

1.1 Type II

In 1957, Abrikosov investigated the effects of a large κ. The radically different behaviour prompted the need for a new category, named type II superconductors. He found that, there was a behaviour change caused by two values of the external field (not just one). While the field was weak the material behaved as any other superconductor and a strong field (over Hc_2) would break the superconductive behaviour. However, after a threshold (Hc_1), the external field would penetrate the material in the form of vortices in the bulk of the material. As the field grows, so did the number of vortices, until reaching Hc_2, which eliminated all superconductive behaviour. This was called the mixed state, and its vortices are the subject of this work [1, 6]. Abrikosov thought that these vortices arranged themselves in a square lattice [6], however, further examination by Kleiner, Roth, and Autler proved that the hexagonal lattice is more stable [1, 7]. Afterward, Essmann and Träuble provided direct observation of the hexagonal lattice [8]. Despite his original mistake, the hexagonal lattice of the mixed state is called the Abrikosov lattice. Figure 1 depicts a type II superconductor in the mixed state.

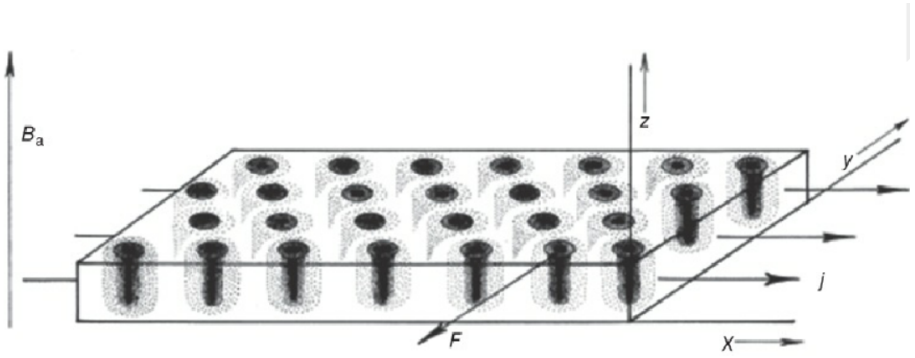

Figure 1: Mixed state of the bulk of a rectangular superconductor under a transport current of density j. Image taken directly from Fig 5.7 in [3]

1.2 Vortices

It is important to understand the causes of movement of vortices in the mixed state in the geometry of a rectangular type II superconductor. The material studied is assumed to be "thick", the thickness of the material, d, is large compared to λ [9]. Since, thin superconductors are known to lose properties (Meissner effect) and have a different vortex-vortex interaction [5, 10]. All calculations will be considered far away from the vortex centre. This project only considers superconductors with vortices that have small radii, in comparison to λ. This allows for the vortices to be approximated as point-like in simulations.

1.2.1 Interactions between vortices

This interaction is responsible for the vortices forming a hexagonal lattice. These forces can be calculated by considering the free energy contribution from two vortices separated by r_{12} [1]. The force is

$$F_{12} = \frac{\Phi_0^2}{2\pi^2\mu_0\lambda^3} K_1(\frac{r_{12}}{\lambda}) \tag{3}$$

where Φ_0 is the total flux carried by a unit cell ($\Phi_0 = hc/2e$), and K_1 is the modified Bessel function of the second kind. The force is repulsive and acts in the radial direction r_{12} [5].

1.2.2 Driving forces

Applying a current **J** to the superconductor results in a Lorentz force (F_D) perpendicular to both the applied current and external magnetic field, which is called the driving force.

Of interest to this project is the application of a driving force in a superconducting narrow channel (SCNC). Introduced by A. Pruymboom et al. in 1988 [11], a channel is made by layering two different superconductors, and removing a narrow channel off the top layer, which exposes the lower superconductive layer [5]. This results in weak-pinned vortices in the channel being surrounded by strong-pinned ones [11]. In this environment, the strong-pinned vortices form a periodic potential, which traps the weak-pinned vortices. However, a strong enough driving force can overcome the potential and induce constant velocity in the weak-pinned vortices. The lowest driving force that is able to overcome the potential is called the critical sheering force. The behaviour of the time averaged velocity of a chain of vortices with respect to the driving force was found analytically [5]. This makes plotting the behaviour a good benchmark test, and calculating the critical sheering force a good way to ensure that the constants are appropriate. To achieve this, it is important to note that introducing a current perpendicular to the channel results in a driving force (F_{DC}) along it. This means that the final force experienced by a vortex in a driven channel is $F_{12} + F_{DC}$.

1.2.3 Temperature dependent displacement

As temperature increases, the vortices gain energy, which transfers to unpredictable movement. If the temperature is increased, there will come a point when the ordered lattice breaks. This process is called melting [5, 12, 13].

This is controlled by a thermostat $\chi(T)$, which is added to the total force. Therefore, the final force defining the movement of a vortex is

$$F = F_{12} + F_{DC} + \chi(T). \tag{4}$$

2 Simulations

In order to simulate vortices, they are approximated as point-like particles under the effect of the forces aforementioned. Therefore, the equation of motion is

$$m^*\ddot{r} = F - \eta\dot{r}$$

, where η is the viscous drag coefficient. If the vortices are not in a stable state, a vortex will move by δx in time δt, where $\delta x = \int_t^{t+\delta t} F/\eta \; dt$. By applying the Euler technique

$$\delta x = \delta t \; \frac{F}{\eta} \tag{5}$$

, but the error of the Euler method is directly proportional to δt, so the time increments must be small. In all simulations $\eta = \lambda = 1$ and $\delta t < 10^{-2}$.

2.1 Benchmarks

2.1.1 Rectangular surface with double periodic boundaries

This test simulates the bulk of a large superconductor. In order for edge effects to be neglected, the double periodic boundaries are employed. It does not include driving forces or thermal effects, so $F = F_{12}$. This test has two stages. First, the stability of the ground state is checked by initializing a hexagonal lattice of vortices and letting them interact. After successfully proving the stability of the lattice, 100 vortices were initialized at random positions as depicted in fig. 2a. After T = 10000 time steps of $\delta t = 10^{-3}$ the system settled into the state shown in fig.2b.

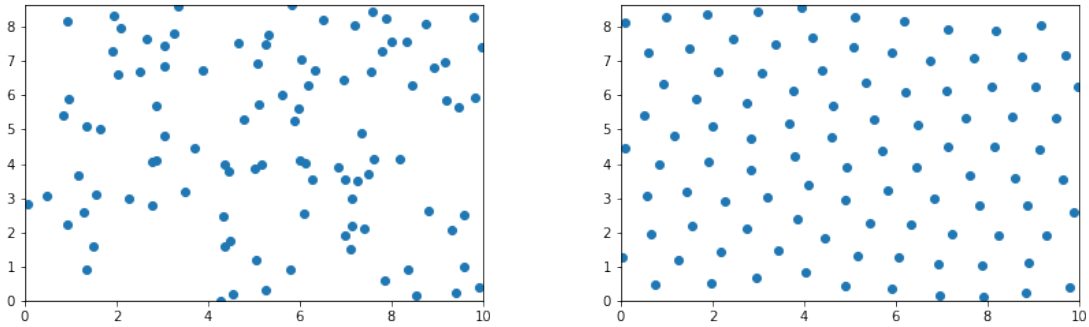

(a) Initialization (b) Final state

Figure 2: The first benchmark test with randomly initialized vortices before and after interacting for T time steps. Each blue dot represents the position of a vortex.

2.1.2 Superconducting narrow channel

This benchmark consists of calculating the critical shear force, and graphing the average velocity and driving force in order to check for appropriate constants and good implementation, respectively. Thermal effects are not considered in this simulation, so $F = F_{12} + F_{DC}$. the channel considered has one vortex chain and periodic boundaries perpendicular to the length of the channel. The pinned vortices are in a perfect hexagonal lattice, therefore, they form a periodic potential that can be calculated at a general position (x,y). To do so, one can consider the potential of a line of N vortices separated by a constant length $V_L = \sum^N K_0(\sqrt{(x + a_x n)^2 + y^2})$. Then, a Fourier transform is applied, and standard Gaussian integrals are identified. The potential is transformed back to real space, and summed in the vertical direction over $V_L(x+ma_x/2; y+ma_y/2)$. This results in the potential of a semi-infinite lattice V_{SIL}. Since the channel is formed by two semi-infinite lattices divided by a vortex chain $V_C(x, y) = V_{SIL}(x, y) + V_{SIL}(x, w - y)$, where w is the width of the channel [5]. Note that in an Abrikosov lattice $a_x = 1$ and $a_y = \sqrt{3}/2$. Also, the channel contains one chain, so $w = 2a_y$, and since the channel remains symmetric in y even after adding the driving force, $y = const. = a_y$. Therefore,

$$V_C(x) = 2\pi \sum_{n=-\infty}^{\infty} \alpha_n e^{-2\pi i n x} e^{-Q_n \sqrt{3}/2} = V_{C0} + C \sum_{n=1}^{\infty} \alpha_n cos(2\pi n x).$$

This potential converges very fast, so it is appropriate to only consider the first term so $V_C = V_{C0} + C_1 cos(2\pi x)$. The force exerted by the lattice on the channel is $F_L = \frac{dV_C}{dx} = -C_F sin(2\pi x)$. To calculate vortex movement the final force $F = F_L + F_{DC}$, where F_{DC} ranges from 0 to 0.1 is used. It runs for 10^7 time steps, after each change in F_{DC} the system is left to stabilize for 10^5 steps. Afterwards, the velocity of each vortex is stored for the reminder of steps under that driving force. One time step before increasing the driving force, the stored velocities are averaged and stored for plotting. Figure 3a is the resulting graph. Figure 3b is the analytic result of the same quantities. The general behaviour is in agreement between the two, however smaller changes in F_DC could improve it. The dashed line in figure 3a represents the critical shear force, which the simulation agrees with. This is important since no other behaviour studied up to now is affected by constants, so having the right critical shear shows that constants are in agreement with reality.

2.2 Main project

As the general behaviour of the simulations agrees with previous work, it can be used as a basis for melting the mixed state. This involves no driving force, but its implementation was important in checking constants. The project involves studying a rectangular surface with double periodic boundaries, just as the first benchmark test. However, thermal effects are introduced via an Andersen thermostat. An indication function is used to choose which vortices are dislocated each time step. Then, a 2D Gaussian is

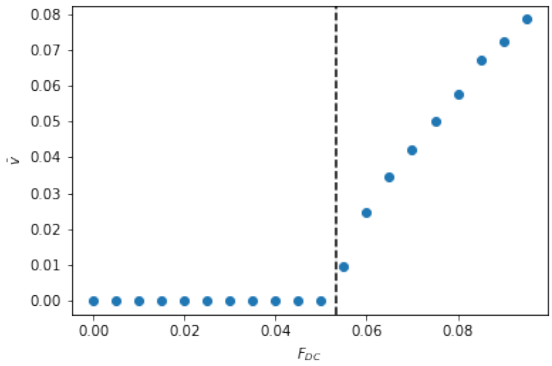

(a) Simulated graph, the dashed line marks the expected value of the critical shear.

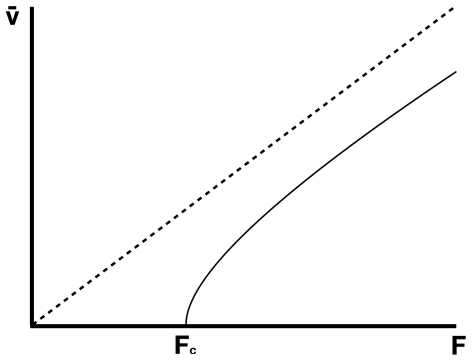

(b) Analytically calculated graph, taken from Fig.6.2 [5]
.

Figure 3: Comparison of simulated and analytical graph of average velocity and driving force.

multiplied by the square root of temperature to result in χ, the force on the vortex due to temperature. This thermostat was successfully implemented.

Further work involves calculating the hexatic order parameter

$$\Psi_H = |\langle \frac{1}{N_v} \sum_{j=1}^{N_v} \frac{1}{z_j} \sum_{k=1}^{z_j} e^{i6\theta_{jk}} \rangle|^2 [12]$$

, where N_v is the number of vortices, z_j is the number of nearest neighbours, and θ_{jk} is the angle between the vortex and its neighbour. Finding the nearest neighbours will be done by Delaunay triangulation. The parameter will be used to label systems as ground state, $\Psi_H = 1$, or melted, $\Psi_H = 0$, These systems will be transformed in Fourier space to reduce the amount of data the classification algorithm needs for an accurate result. Finally, a classification algorithm will be trained to recognize a system in the ground state or in the melted state. This will then be used to analyse intermediary stages. It can become a valuable tool in understanding the behaviour of vortices and the melting of the mixed state.

References

[1] Tinkham M. Introduction to superconductivity / Michael Tinkham. 2nd ed. Mineola, N.Y.: Dover Publications; 2004. Book Title: Introduction to superconductivity / Michael Tinkham.

[2] Poole CP. Superconductivity / Charles P. Poole, Jr., Ruslan Prozorov, Horacio A. Farach, Richard J. Creswick. 3rd ed. Elsevier insights. Amsterdam: Elsevier Science; 2014. Book Title: Superconductivity / Charles P. Poole, Jr., Ruslan

Prozorov, Horacio A. Farach, Richard J. Creswick. Available from: https://www-sciencedirect-com.ezproxye.bham.ac.uk/book/9780124095090/superconductivity.

[3] Kleiner R, Buckel W, Huebener R. Superconductivity: An Introduction. Weinheim, GERMANY: John Wiley & Sons, Incorporated; 2016. Available from: http://ebookcentral.proquest.com/lib/bham/detail.action?docID=4044603.

[4] London F, London H, Lindemann FA. The electromagnetic equations of the supraconductor. Proceedings of the Royal Society of London Series A - Mathematical and Physical Sciences. 1935 Mar;149(866):71-88. Publisher: Royal Society. Available from: https://royalsocietypublishing.org/doi/10.1098/rspa.1935.0048.

[5] Gartlan JA. Novel excitations in driven vortex channels in a superconductor, and solitary waves of light and atoms in photonic crystal fibres [PhD]. University of Birmingham; 2020. Available from: https://etheses.bham.ac.uk/id/eprint/9918/.

[6] Abrikosov A. On the Magnetic Properties of Superconductors of the Second Group. Soviet Physics JETP. 1957 Dec;5.

[7] Kleiner WH, Roth LM, Autler SH. Bulk Solution of Ginzburg-Landau Equations for Type II Superconductors: Upper Critical Field Region. Physical Review. 1964 Mar;133(5A):A1226-7. Available from: https://link.aps.org/doi/10.1103/PhysRev.133.A1226.

[8] Essmann U, Träuble H. The direct observation of individual flux lines in type II superconductors. Physics Letters A. 1967 May;24(10):526-7. Available from: https://www.sciencedirect.com/science/article/pii/0375960167908195.

[9] Pearl J. Current distribution in superconducting films carrying quantized fluxoids. Applied Physics Letters. 1964 Aug;5(4):65-6. Publisher: American Institute of Physics. Available from: https://aip.scitation.org/doi/abs/10.1063/1.1754056.

[10] Brandt EH. Vortex-vortex interaction in thin superconducting films. Physical Review B. 2009 Apr;79(13):134526. ArXiv: 0904.1436. Available from: http://arxiv.org/abs/0904.1436.

[11] Pruymboom A, Kes PH, van der Drift E, Radelaar S. Flux-line shear through narrow constraints in superconducting films. Physical Review Letters. 1988 Apr;60(14):1430-3. Publisher: American Physical Society. Available from: https://link.aps.org/doi/10.1103/PhysRevLett.60.1430.

[12] Spencer S, Jensen HJ. Absence of translational ordering in driven vortex lattices. Physical Review B. 1997 Apr;55(13):8473-81. Publisher: American Physical Society. Available from: https://link.aps.org/doi/10.1103/PhysRevB.55.8473.

[13] Guillamón I, Suderow H, Fernández-Pacheco A, Sesé J, Córdoba R, De Teresa JM, et al. Direct observation of melting in a two-dimensional superconducting vortex lattice. Nature Physics. 2009 Sep;5(9):651-5. Bandiera_abtest: a Cg_type: Nature Research Journals Number: 9 Primary_atype: Research Publisher: Nature Publishing Group. Available from: https://www.nature.com/articles/nphys1368.